

Spatio-Semantic ConvNet-Based Visual Place Recognition

Luis G. Camara and Libor Přeučil

Czech Institute of Informatics, Robotics and Cybernetics, Czech Technical University in Prague, Prague, Czech Republic

luis.gomez.camara@cvut.cz

Abstract—We present a Visual Place Recognition system that follows the two-stage format common to image retrieval pipelines. The system encodes images of places by employing the activations of different layers of a pre-trained, off-the-shelf, VGG16 Convolutional Neural Network (CNN) architecture. In the first stage of our method and given a query image of a place, a number of top candidate images is retrieved from a previously stored database of places. In the second stage, we propose an exhaustive comparison of the query image against these candidates by encoding semantic and spatial information in the form of CNN features. Results from our approach outperform by a large margin state-of-the-art visual place recognition methods on five of the most commonly used benchmark datasets. The performance gain is especially remarkable on the most challenging datasets, with more than a twofold recognition improvement with respect to the latest published work.

I. INTRODUCTION

In the field of mobile robotics and particularly in applications requiring long-term navigation and localization [1, 2], the problem of *Visual Place Recognition* (VPR) is a fundamental one and still an open computer vision research topic [3, 4, 5, 6]. Navigation systems used by mobile robots are typically based on *Simultaneous Localization And Mapping* (SLAM) approaches [7, 8, 9]. In long-term SLAM implementations, the task of determining whether a robot is located at a previously visited place becomes a basic requirement. This is known as *loop closure* and is typically solved by VPR [4, 10, 11] in image-based systems.

Visual place recognition is however a challenging problem, especially in uncontrolled outdoors environments and over long periods of time. Images captured by a robot at a specific location can differ significantly with respect to those captured on a first pass through the same location. This is due to environmental factors such as differences in the season of the year, changing weather conditions, day-night cycles, light variations during the day and/or purely geometric aspects such as changes in viewpoint between two traverses.

Loop closure is typically approached in the literature by using Bag of (visual) Words (BoW) models [4, 11, 12] or the closely related VLAD [5, 13, 14] and Fisher vectors [15, 16]. These approaches aggregate robust image features into previously created dictionaries of visual words, leveraging the resulting compact representations for the creation and fast query of image databases. Nonetheless, these models are strictly content-based and do not take into account spatial

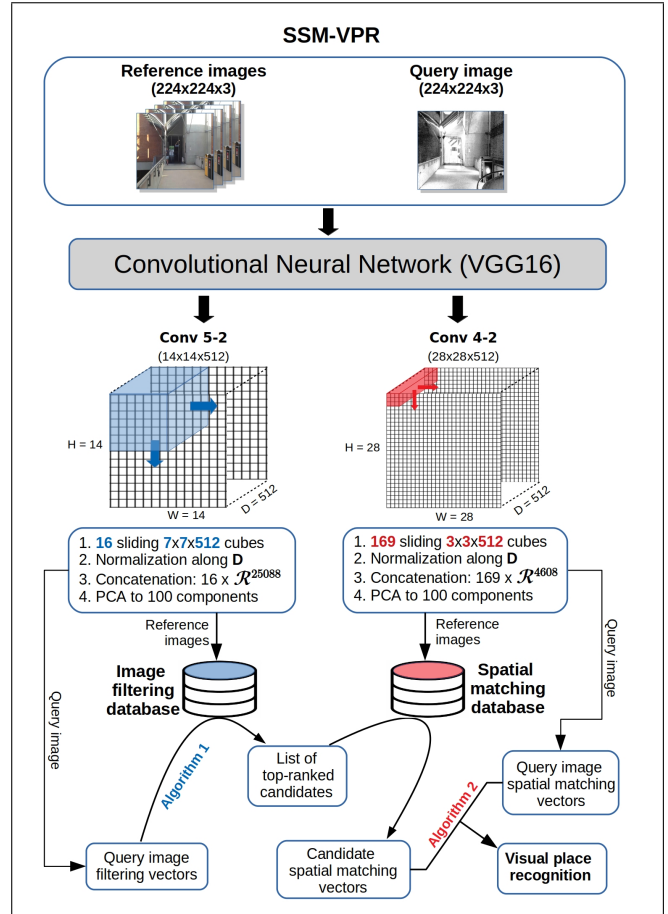


Fig. 1: Workflow of our Semantic and Spatial Matching Visual Place Recognition (SSM-VPR) system.

relationships between image features. It is for this reason that they are usually fairly robust to viewpoint changes but suffer from problems such as perceptual aliasing [17].

More recently, inspired by the great success of Convolutional Neural Networks (CNN) in several computer vision tasks, a number of authors have employed the activations of some CNN layers to create image representations suitable to tackle the VPR problem [5, 10, 18, 19, 20, 21, 22, 23, 24]. By discarding the fully connected layers of CNNs and using the output of their middle and later convolutional layers instead, it has been shown that it is possible to encode rich semantic information that may be robust to several image changes. Yet, most authors do not explicitly take into consideration the spatial locations of the activations and aggregate them

into orderless BoW models or simply concatenate them into high-dimensional spaces.

In this work, we take a step forward and approach the VPR problem by focusing not only on the semantics provided by CNN features but also, and very importantly, on the geometric relationships between these features in images. Some recent works [25, 26] have in fact considered CNNs to geometrically match images, although outdoor VPR under challenging conditions has not been explicitly addressed. The main contribution of our work is the implementation and evaluation of a VPR system based on a very simple yet effective CNN-based spatial matching stage, which is preceded by a baseline image retrieval stage, also based on CNN features. At present, we focus on visual place recognition performance rather than optimizing computational complexity and show that our approach outperforms by a large margin previously published results on five benchmark image datasets [23, 24].

The remaining of this paper is structured as follows. In Section II we review published work related to the VPR problem and put our work into context. Our methodology is presented in Section III, characterizing our ground truth and describing the two stages of our system. In Section IV, experimental results are presented, compared with the state-of-the-art and discussed. Finally, Section V is left to conclusions and to describe our line of work in the future.

II. RELATED WORK

Previous to the resurgence of CNN models [27], commonly followed computer vision approaches in VPR employed handcrafted robust features such as SIFT [28], SURF [28], ORB [29], etc. to represent images, encoding them into BoW-like models by using pre-trained dictionaries of visual words [4, 11, 13, 30]. In recent years, however, CNN-based features have shown their superiority in many computer vision tasks [31, 32, 33], including VPR. Hence, latest published work in VPR is mostly based on CNN image representations and also our main focus in this section.

Some of the first works utilizing CNN descriptors in the VPR problem can be found in [18, 19], where the authors used pre-trained networks and explored the capabilities of different layers on different aspects of the place recognition task. They observed that later layers held more semantic information and therefore were more robust under conditions of large viewpoint variance, whereas middle layers were less affected by appearance changes such as illumination. Hou et al. [10] also investigated the performance of CNN intermediate layers as image descriptors and concluded that they were faster to compute and achieved similar or better performance compared to handcrafted image descriptors. In [20], the authors extracted potential landmarks from images using the *Edge Boxes* [34] object proposal algorithm and tried to find the best matches between them. They significantly improved recognition performance, although the detector itself imposed a heavy computational load. Arroyo et al. [21] proposed a methodology where the activations of multiple convolutional layers were fused by concatenation, compression and binarization, showing better performance

than traditional image descriptors and even some baseline CNN approaches.

Instead of using pre-trained architectures, some authors have trained their networks specifically for the VPR task. For instance, [22] created a large dataset of places and trained a network that interpreted VPR as a classification problem, achieving an average 10% increase in performance over other approaches. Of great relevance in VPR is the work of Arandjelović et al. [5], who designed a CNN architecture, NetVLAD, which incorporated a VLAD layer and could be trained in an end-to-end fashion for the place recognition task. Their results on some very challenging datasets were remarkable, significantly outperforming state-of-the-art works based on pre-trained CNNs.

Recently, following the success of region-based approaches, Chen et al. [23] created a system that used a late convolutional layer as a landmark detector and an earlier one to create local descriptors to match the detected landmarks. Their system showed improved recognition under strong viewpoint and condition variations. One of the latest published work in VPR is that of Kaliq et al. [24]. By detecting regional features and VLAD-encoding them, they created a lightweight pipeline that outperformed the 2-layer approach of [23].

More in line with our two-stage methodology, some authors have in fact considered geometric post-verification of shortlisted locations [35, 36], resulting in a significant boost in recognition performance. These authors focused however on handcrafted features. To the best of our knowledge, a system that takes advantage of the power of CNN features for both retrieval and geometric verification in the context of VPR is lacking in the literature.

III. PROPOSED METHODOLOGY

We consider the problem of VPR as an *image retrieval* one [5, 37, 38], which is usually divided into (i) a *filtering stage* and (ii) a *re-ranking* stage [39]. During stage (i) and given a *query image*, a whole database of *reference images* is searched and a number of top-ranked candidates retrieved according to some similarity or distance metric. In stage (ii), the candidates are compared with the query image in a more exhaustive fashion and re-ranked to give an ordered list of the best matches. The place recognition problem then reduces to choosing the top match from the re-ranked list.

In our approach, we follow this two-stage structure and encode our images using two different layers of the VGG16 CNN architecture [31], one for each stage. We employed the VGG16 network pre-trained on the Places205 dataset [40], which is conceptually closer to VPR than the more commonly used ImageNet dataset [41], oriented towards object recognition (we advance that it is our plan to explore in the future end-to-end trainable networks such as NetVLAD). For convenience, we called our approach SSM-VPR (Semantic and Spatial Matching Visual Place Recognition).

The structure of our pipeline is illustrated in Figure 1. Reference and query images are passed through the network and the activations of two specific layers, *conv5-2* and

conv4-2, stored for processing. In the case of reference images, permanent databases are created for later comparison against query images. Our choice of layers is based on experimentation. Layer *conv5-2* contains less spatial resolution (14×14 activations per feature map) although, being one of the latest layers in the network, provides strong semantics. This materializes into better performance when used in the image filtering stage. On the other hand, layer *conv4-2* contains twice the spatial resolution. It is therefore more suitable for geometrical comparisons between images while still producing features that are robust enough to image changes. Each layer contains $D=512$ feature maps and a total of $H \times W \times D$ activations, where the first two dimensions correspond to spatial locations. All images were scaled to size $224 \times 224 \times 3$ RGB.

Before describing the two stages of our system in more detail, we first comment on the way our ground truth is defined, since this directly affects the presented recognition results.

A. Ground truth and distance tolerance

During the evaluation of a VPR system, it must be decided whether the guessed location of a query image is a true positive or not. Since the definition of a place is somehow fuzzy, a distance tolerance is highly convenient for this task. We have adopted from [5, 13, 42] the criterion that a query image is deemed as a true positive when its ground truth location is within 25 m from the guessed location.

The datasets employed throughout this work consist of pairs of image sequences of the same traverse but under different conditions (see Section IV-B). They have been tagged so that frames corresponding to the same place in both traverses contain the same numerical label. This allows for the use of frame tolerance instead of distance in the evaluation of true positives. We propose to find the optimal frame tolerance in the datasets by directly looking at the recognition performance of the system as the tolerance is varied. Hence, an analysis of performance vs. frame tolerance is carried out in Section IV.

B. Image filtering stage

We want to make our image filtering stage as robust to viewpoint changes as possible. Using full-image representations can rapidly degrade recognition performance under changes in viewpoint, as large parts of the reference images may be missing in the query image. Several authors have shown that selecting regions of interest can boost recognition performance [20, 23, 24]. Rather than trying to find those regions, we take a brute force approach and spatially scan the feature maps by dividing them into smaller sections.

Based on layer *conv5-2* and as seen in Figure 1, cubes of dimensions $7 \times 7 \times 512$ were defined by sliding along the layer’s horizontal (W) and vertical (H) directions. With a stride size of $s = 2$ activations, the sliding process led to a total of 16 cubes per image. After normalization along the direction of the feature maps, we concatenated the activations in each cube and created 16 vectors of

dimension $7 \times 7 \times 512 = 25088$. Since working in such a high dimensional space is expensive in terms of memory and complexity, we performed dimensionality reduction through Principal Component Analysis (PCA), a common practice when working with CNN features [43].

As it will be shown in Section IV-B and in order to justify our use of PCA, we conducted several experiments on the considered datasets and observed that the recall@25 (the percentage of successfully retrieved images when using a list of candidates of size 25) did not improve above 80 principal components. The criteria of success was that at least one image in the list was close enough to the ground truth, with a tolerance of ± 2 frames. Prudently, we decided to reduce our vectors to $d = 100$ dimensions instead of 80. For each image in the reference dataset, we encoded the convolutional cubes and stored them in an *image filtering database* (IFDB). We did not store any information about the spatial location of the cubes.

The same processing described above was performed on any entering query image. Subsequently, the vectors representing that image were compared one by one against the IFDB and, based on a nearest neighbor distance criterion, the first N candidates were added to a histogram of places. The resulting accumulated histogram of places was then used to extract a list of N top-ranked candidate images (see Algorithm 1 for a pseudo code).

Algorithm 1 Image filtering stage

```

1: Get query image vectors  $\{q_i\}$  ( $16 \times \mathbb{R}^{100}$ ) from conv5_2
2: cand_hist  $\leftarrow$  Initialize histogram of candidate images
3: for  $i = 1$  to 16 do
4:   Find best  $N$  matches of  $q_i$  in IFDB
5:   Update the corresponding  $N$  bins in cand_hist
6: end for
7: Candidate list  $\leftarrow$  Select  $N$  highest bins from cand_hist

```

C. Spatial matching stage

The outcome of the filtering stage is an ordered list of N images that are similar to the query image in a vector distance sense. We want to emphasize the notion that the geometric relationships or spatial constraints among the elements of images are of vital importance in the recognition of a place. We believe humans recognize places by identifying semantic elements in a scene and then finding geometric relationships between them [44]. Following this intuition, we created a matching system based on convolutional features that is able to capture semantic information and at the same time keep track of the spatial relationships between those features.

As can be appreciated from Figure 1, the number of activations in each convolutional cube for layer *conv4-2* is $3 \times 3 \times 512 = 4608$. After normalization, concatenation, PCA compression and the application of a stride of $s = 2$, each image is represented by an array of $13 \times 13 = 169$ vectors in \mathbb{R}^{100} . For each image, we stored those vectors in a *spatial matching database* (SMDB), along with their position in the array. In this fashion, when comparing query and candidate images, it is possible to match both convolutional features

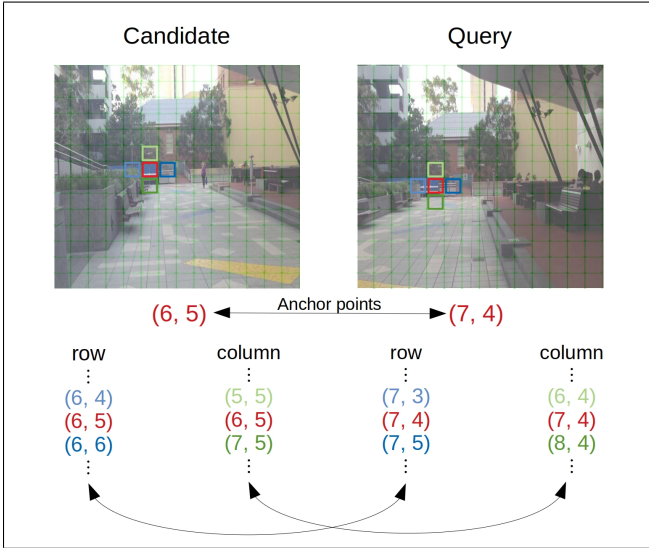


Fig. 2: Illustration of the spatial matching approach for an individual location (square-marked region) within a candidate image.

and their spatial arrangement. In what follows, we provide the main ideas of our spatial matching approach, which are also summarized as pseudo code in Algorithm 2.

We take the list of N candidates provided by the first stage of our system and compare each one of them with the query image. Given a candidate image, we retrieve from the SMDB the collection of vectors $\{c_{i,j}\}$ representing it as well as their locations (i,j) . A spatial consistency check against the query image representation, $\{q_{k,l}\}$, is then performed. This is schematically illustrated in Figure 2, where the grids seen in the two images define the spatial locations of the vectors. Let us focus for instance on position $(6,5)$ for the candidate image, whose vector is denoted by $c_{6,5}$. We start by finding in the query image the best match for $c_{6,5}$, which happens to be at location $(7,4)$ and is denoted by $q_{7,4}$. We call these two locations *anchor points*.

Our spatial matching approach is based on evaluating location consistency of matching vectors in both images with respect to the anchor points. In the figure, if the two example anchors represent the same reality, then we would expect that the best match for the vector on the left-hand side of the candidate’s anchor, $c_{6,4}$, would be $q_{7,3}$ in the query image. Similarly, the best match for the vector on the right-hand side of the anchor, $c_{6,6}$, would be $q_{7,5}$. We continue checking this consistency for the rest of the row in which the anchor is located. As exemplified in Figure 2 and in order to explore the vertical direction, we also check for consistency among the anchor’s column. We carry out the above procedure not only for position $(6,5)$, but for every single position in the candidate image. For each candidate, we accumulate a score counting the number of successfully matched locations over the rows and columns of all positions and store them in a histogram of candidates. Finally, we choose from the histogram the bin with the greatest accumulated score as the place match for the query.

Algorithm 2 Spatial matching stage

```

1:  $candidates \leftarrow$  Get candidate list from Algorithm 1
2:  $\{q_{i,j}\} \leftarrow$  Get query image vectors from  $conv4\_2$ 
3:  $cand\_hist \leftarrow$  Initialize histogram of candidate images
for each: candidate in  $candidates$ 
4:  $\{c_{i,j}\} \leftarrow$  Get candidate vectors from SMDB
5: for all  $i, j \in \{0 \dots 12\}$  do
6:    $q_{k,l} \leftarrow$  Find best match of  $c_{i,j}$  in query image
7:   Set  $(i, j)$  and  $(k, l)$  as anchor points
8:   for  $n = -j$  to  $(12 - j)$  do (scan current row)
9:     if  $q_{k,l+n}$  is best match for  $c_{i,j+n}$  then
10:       Increase candidate bin in  $cand\_hist$ 
11:     end if
12:   end for
13:   for  $m = -i$  to  $(12 - i)$  do (scan current column)
14:     if  $q_{k+m,l}$  is best match for  $c_{i+m,j}$  then
15:       Increase candidate bin in  $cand\_hist$ 
16:     end if
17:   end for
18: end for
19: Select from  $cand\_hist$  the candidate with the highest bin

```

IV. EXPERIMENTS

A. State of the art in VPR

We compared our results with published performance of various VPR approaches. In particular, we considered the recent methods developed in [23] (Region-BoW) and [24] (Region-VLAD) as well as the approaches against which they compared their work (see [23] and [24] for an explanation): *FAB-MAP*, *SeqSLAM*, *AlexNet*, *SUMPOOL*, *MAXPOOL* and *CROSSPOOL*.

B. Datasets

The datasets employed throughout this work are the same or similar to those used by [24] and [23], in an effort to make meaningful comparisons of our results with those of the recent literature. They are summarized in Table I. These

TABLE I: Summary of the datasets used throughout this work

Dataset	Ref. images	Query images
Gardens Point	200 (day-left)	200 (night-right)
Berlin A100	85 (car)	81 (car)
Berlin Halenseestrasse	67 (car)	157 (bicycle)
Berlin Kudamm	201 (bus)	221 (bicycle)
Synthesized Nordland	1415 (summer)	1415 (winter)

datasets have been well described elsewhere and represent a wide range of environments, viewpoint variations and condition changes. We refer the reader for instance to [23, 24, 19, 20] for a more thorough description. The datasets themselves were downloaded as referenced in [24]. Figure 3 shows some examples of the reference and query images for the datasets considered.

C. Results and discussion

Before presenting our recognition results, we justify the choice of ground truth tolerance used in our experiments. Results for the analysis mentioned in Section III-A are presented in Figure 4. They show the recognition precision at 100% recall for $d = 100$ and $N = 50$ when considering



Fig. 3: Same place examples of reference (left) and query (right) images for the datasets considered in this work. Rows are, in descending order, *Gardens Point*, *Berlin A100*, *Halenseestrasse*, *Kudamm* and *Nordland* datasets.

several frame tolerances in the assignment of true positives. Zero tolerance signifies that only those query images whose guessed location is exactly the ground truth are considered true positives.

As can be seen in the figure, relaxing the tolerance quickly translates into an increase in precision. This is because there may be several query images whose guessed place is not exactly the ground truth but fairly close to it and therefore they can be considered as true positives. We also see in the figure that above certain tolerances the performance gain rate becomes both small and constant. This is consistent with the random inclusion of images as true positives due exclusively to larger tolerances but otherwise uncorrelated with the current place. We consider this drop in performance gain as an intrinsic indicator of the spatial limits of a given place and consequently we set the frame tolerance to ± 2 frames. In all datasets, this value meets the distance threshold of 25 m (Section III-A) although for the sake of completeness, we will also provide some results for tolerances of ± 1 and ± 3 frames.

We present in Figure 5 our analysis on the image filtering performance as a function of the number of principal components. The results are given for a recall@25. We clearly see that for all datasets there is no significant gain in recall above around 80-90 components. This allowed us to reduce the CNN feature vectors to 100 dimensions without apparent loss in performance. We also made this assumption for the spatial matching stage (a detailed analysis like the one in the figure will be provided in future work).

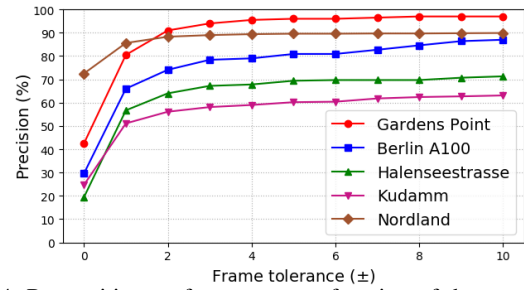


Fig. 4: Recognition performance as a function of the ground truth frame tolerance.

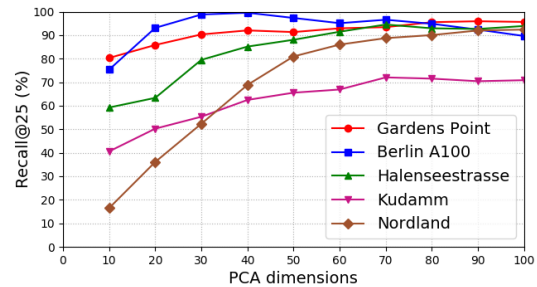


Fig. 5: Effect of the number of dimensions on image filtering performance (recall@25) for layer `block5_conv2`.

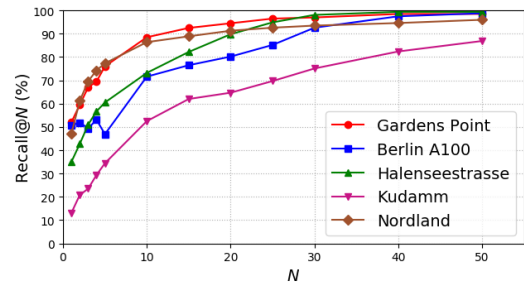


Fig. 6: Recall as a function of the number of candidates N in the image filtering stage.

With the number of dimensions fixed to $d = 100$, we investigated the influence of the candidate list size N on the image filtering recall performance, which is summarized in Figure 6. For $N=1$, the recall can be interpreted as the place recognition performance of layer `conv 5-2`, as only the best candidate is taken into account. The performance of this layer is comparable for instance to CNN methods that use the whole image [19, 20].

As the number of candidates becomes larger, we see that the recall increases rapidly, although the growth progressively slows down for larger values of N . With the exception of the *Kudamm* dataset, which is known to be particularly challenging, the recall is above 95% for all datasets at $N = 50$, justifying the use of this value in our experiments.

We assessed the recognition performance of our two-stage system on the five datasets by evaluating precision-recall curves on them. The resulting curves are shown in Figure 7, where three ground truth frame tolerances are considered for completeness. The curves show that taking a tolerance of ± 1 is suboptimal, as a significant boost in performance is achieved in all cases by increasing it to ± 2 . On the other hand, relaxing this constraint to ± 3 frames only improves performance by a small amount, a fact that

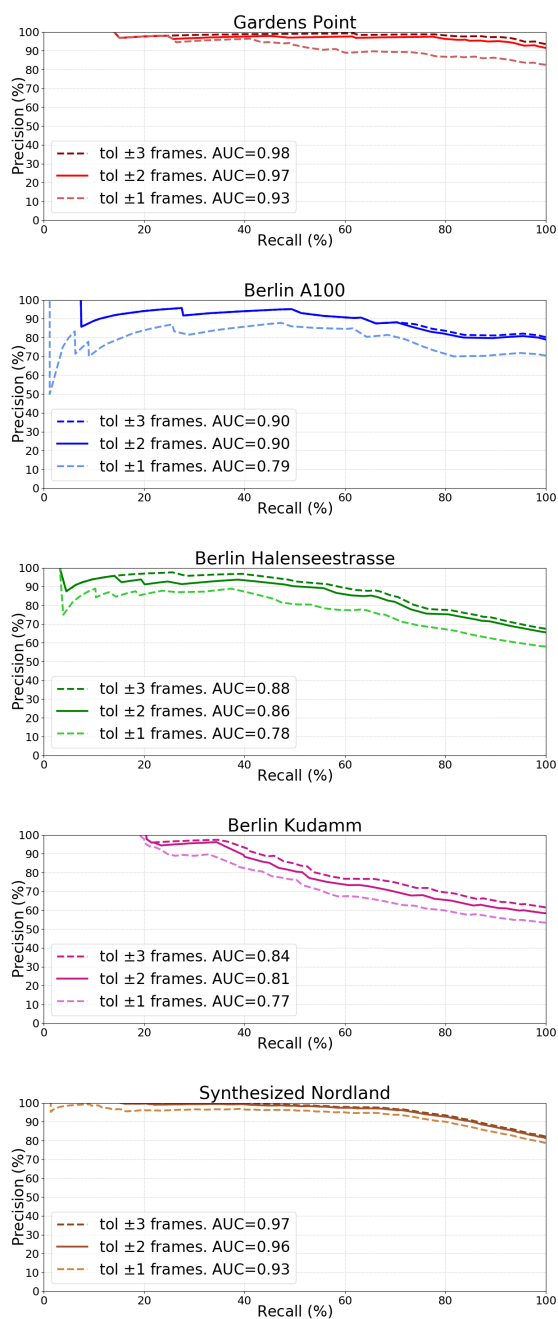


Fig. 7: Precision-recall curves for 3 ground truth frame tolerances.

supports our choice of ± 2 as the standard frame tolerance for the identification of a place.

As can be seen in Figure 8, we compared our recognition results with recent published work [24, 23] by using the Area Under the Curve (AUC) of the precision-recall curves. On the five benchmark datasets considered, we consistently outperformed visual place recognition results. For *Gardens Point* and *Synthesized Nordland*, which represent very strong condition and viewpoint changes for the former and strong condition changes for the latter, we are not too far from perfect performance, with an AUC=0.97. To the best of our knowledge, this level of recognition is unprecedented on these datasets. On the *Synthesized Norland*, the improve-

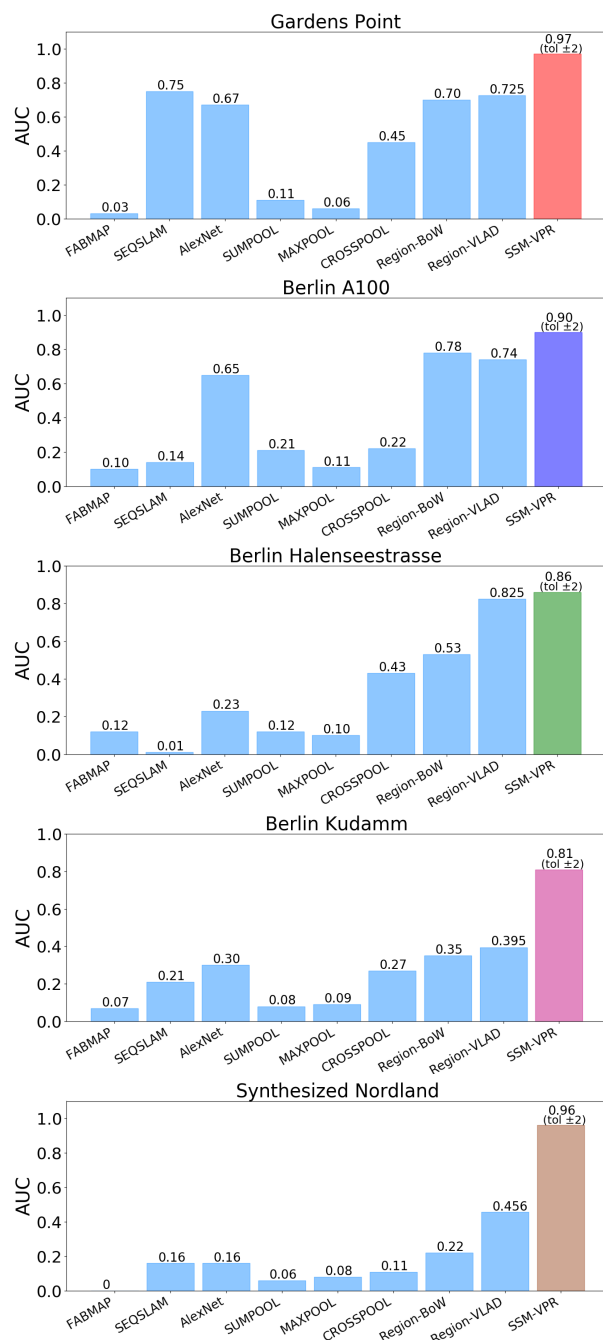


Fig. 8: Area Under the Curve (AUC) of the precision-recall curves.

ment with respect to the state-of-the-art is twofold. It is also remarkable the excellent performance obtained on the *Kudamm* dataset, which is considered in the literature as very challenging. Our results show again a performance that is two times better than the best published results on this dataset. Notice that even if a frame tolerance of ± 1 is considered, we are still on par with published results for the Berlin A100 and Halenseeestrasse datasets and well above for the rest, making clear the superiority of our method.

D. Runtime and memory considerations

At this stage of our work, we have not excessively focused on computational complexity, since our goal was

on recognition performance. The current system can find a place in an average of 1.6 seconds. There exist however several opportunities for reducing this time considerably. The most clear one is to reduce the number of candidate images retrieved in the image filtering stage. Currently, we are using 50 images. A reduction to 15 candidates brings down recognition time to 750 ms and 400 ms for a candidate list of 5 images. With an improvement in our image filtering stage, this could lead to a very competitive recognition system. Regarding the image filtering and spatial matching databases, each image takes approximately 25 kB and 150 kB of disk space, respectively.

V. CONCLUSIONS AND FUTURE WORK

In this work, we have shown that CNN-based image database filtering combined with exhaustive spatial matching of filtered candidates is a successful two-stage approach to the problem of visual place recognition. Following the success of CNNs in several computer vision tasks, we used both their power creating robust representations of images as well as their spatial properties to tackle recognition. We showed that using this combination significantly increases the published recognition performance in commonly used benchmark datasets, some of them highly challenging. It is precisely on these that we achieved the most striking results, with more than a twofold increase in performance with respect to the state-of-the-art.

Our immediate efforts will be focusing on improving the image filtering stage of our system. In particular, we will look at end-to-end trainable architectures such as NetVLAD as the most straightforward approach to both increase the recognition performance and reduce the complexity of the system.

Furthermore, it is our intention to explore alternative spatial matching algorithms, experiment with different image resolutions and introduce knowledge about previously recognized frames to leverage the frame correlation inherent to sequences of images when moving through places.

Finally, we will try to expand the number of datasets in order to include more indoor as well as countryside scenarios and we will start to integrate our system in real robotic applications, with a view on FPGA real-time implementations.

ACKNOWLEDGMENT

This work has been supported by the European Union's Horizon 2020 research and innovation programme under grant agreement No 688117, by the Technology Agency of the Czech Republic under the project no. TE01020197 "Centre for Applied Cybernetics", and by the European Regional Development Fund under the project Robotics for Industry 4.0 (reg. no. CZ.02.1.01/0.0/0.0/15 003/0000470)

REFERENCES

- [1] Gian Diego Tipaldi, Daniel Meyer-Delius, and Wolfram Burgard. "Lifelong localization in changing environments". In: *The International Journal of Robotics Research* 32.14 (2013), pp. 1662–1678.
- [2] Winston Churchill and Paul Newman. "Practice makes perfect? managing and leveraging visual experiences for lifelong navigation". In: *2012 IEEE International Conference on Robotics and Automation*. IEEE, 2012, pp. 4525–4532.
- [3] Stephanie Lowry et al. "Visual place recognition: A survey". In: *IEEE Transactions on Robotics* 32.1 (2016), pp. 1–19.
- [4] Dorian Gálvez-López and Juan D Tardos. "Bags of binary words for fast place recognition in image sequences". In: *IEEE Transactions on Robotics* 28.5 (2012), pp. 1188–1197.
- [5] Relja Arandjelovic et al. "NetVLAD: CNN architecture for weakly supervised place recognition". In: *Proceedings of the IEEE Conference on Computer Vision and Pattern Recognition*. 2016, pp. 5297–5307.
- [6] Akihiko Torii et al. "Visual place recognition with repetitive structures". In: *Proceedings of the IEEE conference on computer vision and pattern recognition*. 2013, pp. 883–890.
- [7] Hugh Durrant-Whyte and Tim Bailey. "Simultaneous localization and mapping: part I". In: *IEEE robotics & automation magazine* 13.2 (2006), pp. 99–110.
- [8] Michael Montemerlo et al. "FastSLAM: A factored solution to the simultaneous localization and mapping problem". In: *Aaai/iaai* 593598 (2002).
- [9] Andrew J Davison. "Real-time simultaneous localization and mapping with a single camera." In: *Iccv*. Vol. 3. 2003, pp. 1403–1410.
- [10] Yi Hou, Hong Zhang, and Shilin Zhou. "Convolutional neural network-based image representation for visual loop closure detection". In: *2015 IEEE international conference on information and automation*. IEEE, 2015, pp. 2238–2245.
- [11] Adrien Angeli et al. "A fast and incremental method for loop-closure detection using bags of visual words". In: *IEEE Transactions on Robotics* (2008), pp. 1027–1037.
- [12] Mark Cummins and Paul Newman. "FAB-MAP: Probabilistic localization and mapping in the space of appearance". In: *The International Journal of Robotics Research* 27.6 (2008), pp. 647–665.
- [13] Akihiko Torii et al. "24/7 place recognition by view synthesis". In: *Proceedings of the IEEE Conference on Computer Vision and Pattern Recognition*. 2015, pp. 1808–1817.
- [14] Stephanie Lowry and Henrik Andreasson. "Lightweight, viewpoint-invariant visual place recognition in changing environments". In: *IEEE Robotics and Automation Letters* 3.2 (2018), pp. 957–964.
- [15] Florent Perronnin et al. "Large-scale image retrieval with compressed fisher vectors". In: *2010 IEEE Computer Society Conference on Computer Vision and Pattern Recognition*. IEEE, 2010, pp. 3384–3391.
- [16] Matthijs Douze, Arnau Ramisa, and Cordelia Schmid. "Combining attributes and fisher vectors for effi-

- cient image retrieval”. In: *CVPR 2011*. IEEE. 2011, pp. 745–752.
- [17] Nishant Kejriwal, Swagat Kumar, and Tomohiro Shibata. “High performance loop closure detection using bag of word pairs”. In: *Robotics and Autonomous Systems* 77 (2016), pp. 55–65.
- [18] Zetao Chen et al. “Convolutional neural network-based place recognition”. In: *arXiv preprint arXiv:1411.1509* (2014).
- [19] Niko Sünderhauf et al. “On the performance of convnet features for place recognition”. In: *arXiv preprint arXiv:1501.04158* (2015).
- [20] Niko Sünderhauf et al. “Place recognition with convnet landmarks: Viewpoint-robust, condition-robust, training-free”. In: *Proceedings of Robotics: Science and Systems XII* (2015).
- [21] Roberto Arroyo et al. “Fusion and binarization of CNN features for robust topological localization across seasons”. In: *2016 IEEE/RSJ International Conference on Intelligent Robots and Systems (IROS)*. IEEE. 2016, pp. 4656–4663.
- [22] Zetao Chen et al. “Deep learning features at scale for visual place recognition”. In: *Robotics and Automation (ICRA), 2017 IEEE International Conference on*. IEEE. 2017, pp. 3223–3230.
- [23] Zetao Chen et al. “Only look once, mining distinctive landmarks from convnet for visual place recognition”. In: *2017 IEEE/RSJ International Conference on Intelligent Robots and Systems (IROS)*. IEEE. 2017, pp. 9–16.
- [24] Ahmad Khaliq et al. “A Holistic Visual Place Recognition Approach using Lightweight CNNs for Severe ViewPoint and Appearance Changes”. In: *arXiv preprint arXiv:1811.03032* (2018).
- [25] Ignacio Rocco, Relja Arandjelovic, and Josef Sivic. “Convolutional neural network architecture for geometric matching”. In: *Proceedings of the IEEE Conference on Computer Vision and Pattern Recognition*. 2017, pp. 6148–6157.
- [26] Hajime Taira et al. “InLoc: Indoor visual localization with dense matching and view synthesis”. In: *Proceedings of the IEEE Conference on Computer Vision and Pattern Recognition*. 2018, pp. 7199–7209.
- [27] Suraj Srinivas et al. “A taxonomy of deep convolutional neural nets for computer vision”. In: *Frontiers in Robotics and AI* 2 (2016), p. 36.
- [28] David G Lowe et al. “Object recognition from local scale-invariant features.” In: *iccv*. Vol. 99. 2. 1999, pp. 1150–1157.
- [29] Ethan Rublee et al. “ORB: An efficient alternative to SIFT or SURF.” In: *ICCV*. Vol. 11. 1. Citeseer. 2011, p. 2.
- [30] David Filliat. “A visual bag of words method for interactive qualitative localization and mapping”. In: *Proceedings 2007 IEEE International Conference on Robotics and Automation*. IEEE. 2007, pp. 3921–3926.
- [31] Karen Simonyan and Andrew Zisserman. “Very deep convolutional networks for large-scale image recognition”. In: *arXiv preprint arXiv:1409.1556* (2014).
- [32] Ross Girshick et al. “Rich feature hierarchies for accurate object detection and semantic segmentation”. In: *Proceedings of the IEEE conference on computer vision and pattern recognition*. 2014, pp. 580–587.
- [33] Vijay Badrinarayanan, Alex Kendall, and Roberto Cipolla. “Segnet: A deep convolutional encoder-decoder architecture for image segmentation”. In: *IEEE transactions on pattern analysis and machine intelligence* 39.12 (2017), pp. 2481–2495.
- [34] C Lawrence Zitnick and Piotr Dollár. “Edge boxes: Locating object proposals from edges”. In: *European conference on computer vision*. Springer. 2014, pp. 391–405.
- [35] Mark Cummins and Paul Newman. “Appearance-only SLAM at large scale with FAB-MAP 2.0”. In: *The International Journal of Robotics Research* 30.9 (2011), pp. 1100–1123.
- [36] César Cadena et al. “Robust place recognition with stereo sequences”. In: *IEEE Transactions on Robotics* 28.4 (2012), pp. 871–885.
- [37] Torsten Sattler et al. “Large-scale location recognition and the geometric burstiness problem”. In: *Proceedings of the IEEE Conference on Computer Vision and Pattern Recognition*. 2016, pp. 1582–1590.
- [38] Eva Mohedano et al. “Bags of local convolutional features for scalable instance search”. In: *Proceedings of the 2016 ACM on International Conference on Multimedia Retrieval*. ACM. 2016, pp. 327–331.
- [39] Giorgos Toliás, Ronan Sifre, and Hervé Jégou. “Particular object retrieval with integral max-pooling of CNN activations”. In: *arXiv preprint arXiv:1511.05879* (2015).
- [40] Bolei Zhou et al. “Learning deep features for scene recognition using places database”. In: *Advances in neural information processing systems*. 2014, pp. 487–495.
- [41] Jia Deng et al. “Imagenet: A large-scale hierarchical image database”. In: *2009 IEEE conference on computer vision and pattern recognition*. Ieee. 2009, pp. 248–255.
- [42] Relja Arandjelović and Andrew Zisserman. “DisLocation: Scalable descriptor distinctiveness for location recognition”. In: *Asian Conference on Computer Vision*. Springer. 2014, pp. 188–204.
- [43] Ken Chatfield et al. “Return of the devil in the details: Delving deep into convolutional nets”. In: *arXiv preprint arXiv:1405.3531* (2014).
- [44] Kevin Lynch. *The image of the city*. Vol. 11. MIT press, 1960.